ANALYSIS OF THE TRANSMUTATION OF LONG LIVED FISSION PRODUCTS USING AN ACCELERATOR

A Thesis

by

JASON ALAN HEARNE

Submitted to the Office of Graduate and Professional Studies of
Texas A&M University
in partial fulfillment of the requirements for the degree of

MASTER OF SCIENCE

Chair of Committee,	Pavel V. Tsvetkov
Committee Members,	Sean M. McDeavitt
	Che Ming Ko
Head of Department,	Yassin A. Hassan

May 2015

Major Subject: Nuclear Engineering

ABSTRACT

The aim of this study is to analyze the transmutation of Long Lived Fission Products (LLFPs) using an accelerator based system. The seven LLFP's are investigated based upon their decay mechanics, yields from fission, and neutron absorption cross sections to select potential target nuclides. MCNPX is the primary modeling tool used. Infinite targets are modeled to determine dependence on the energy of the incident beam. Finite targets containing only nuclides to be transmuted are modeled to compare different LLFPs and finalize the target nuclide selection of ^{99}Tc. Custom cross sections are produced in MCNPX in order to model a target containing other materials and multiple regions. A cylindrical target design is decided upon where the ^{99}Tc content and the dimensions of the target are varied to improve transmutation characteristics. The final target design contains 131 kg of ^{99}Tc mixed with lead in a cylindrical target with a radius of 40 cm and a length of 120 cm, with a cylindrical hole with a 10 cm radius extending 30 cm into the technetium-lead region and a cylindrical graphite reflector region extending 40 cm radially from the target, 50 cm from the front of the target and 80cm from the back of the target. The incident particle energy requirement per transmutation is 56.9 MeV. Using a 1200 MeV proton beam with a power of 2.4 MW (the rate at which the kinetic energy of protons enters the target), the transmutation rate obtained under continuous operation is 1.36 kg/year, corresponding to an initial effective halflife of 66.7 years.

ACKNOWLEDGEMENTS

I would like to thank my committee chair, Dr. Tsvetkov and my committee members, Dr. McDeavitt and Dr. Ko for their support of my project.

I would also like to thank the members of the MCNP help forum and Dr. Chirayath for their assistance with my MCNP modeling.

Finally, thanks to my mother and father for their encouragement and to my wife for her patience and love.

NOMENCLATURE

LLFP	Long Lived Fission Product
MLFP	Medium Lived Fission Product

TABLE OF CONTENTS

Page

LIST OF FIGURES

Page

LIST OF TABLES

Page

1. INTRODUCTION

1.1 General overview of fission products and spent nuclear fuel

Fissioning a heavy nucleus will result in the production of two or more fission fragments, some neutrons, and other particles. A wide range of fission products can be formed and the yields of each specific fission product depend upon the nucleus fissioning and the energy of the incident particle causing the fission. For neutron induced fissions at neutron energy levels present in a reactor, the most probable fission path forms two nuclei with masses approximately equal to 1/3 and 2/3 of the initial nucleus's mass. Increasing neutron energy will skew the probability towards an equal splitting.

Heavy nuclides that are stable or long lived enough to be found naturally are neutron rich, such as ^{235}U, with 92 protons and 143 neutrons; so that the strong force can successfully hold the nucleus together, while lower Z materials tend to be stable with a neutron to proton ratio much closer to 1. Thus, when a heavy nuclide is fissioned, the fission products will generally be unstable due to an over abundance of neutrons. The neutron rich fission products decay primarily by beta emission until a stable nuclide is formed. Some fission products with higher amounts of excess energy will decay by neutron emission, and are referred to delayed neutron precursors. Nearly every fission product is initially very radioactive and quickly decays into a daughter product.

The halflife of a given radioactive nuclide is determined by quantum mechanical nuclear shell mechanics, and is governed by the probability of the escaping particle quantum tunneling through the barriers in order to decay into the more stable daughter nuclide. All spontaneous decays are energetically favorable, and the amount of excess

energy released in the decay is known as the decay energy. Nuclides with higher decay energies will generally decay faster than those with lower decay energies, but other effects specific to the nuclide also play a role. Therefore, the high energy decays will usually happen more quickly, while the lower energy decays have the potential to be much slower, resulting in halflives of hundreds of thousands of years.

Most fission products have decay chains that quickly reach stability, but there are seven long lived fission products (LLFP's) and another seven medium lived fission products (MLFP's). The LLFP's have halflives ranging from 210,000 years to 15.7 million years; while the MLFP's all have halflives shorter than 100 years.

There are two primary components of spent nuclear fuel that contribute to its radioactivity: fission products and actinides. Heavy nuclei such as uranium 238 may absorb a neutron without fissioning to form a new nucleus. This nucleus may decay or absorb more neutrons to form other nuclei. All actinides have the potential to fission, but many do not do so readily in thermal reactors. Higher actinides are too large to be stable and have either spontaneous fission or alpha emission in their decay chains, generally undergoing multiple alphas and betas before reaching stability. The halflives of actinides present in spent fuel range from very short to billions of years, with no large gaps like the fission products. While actinides are responsible for a larger portion of the heat loading of spent fuel, fission products can be more volatile and chemically reactive. Also, for the spent fuel in a typical pressurized water reactor [1], fission products contribute more to the total activity than actinides initially until about 170 years have passed and again from 120,000 to 4 million years, due to the presence of

medium and long lived fission products. The comparative activities can be seen in Figure 1.

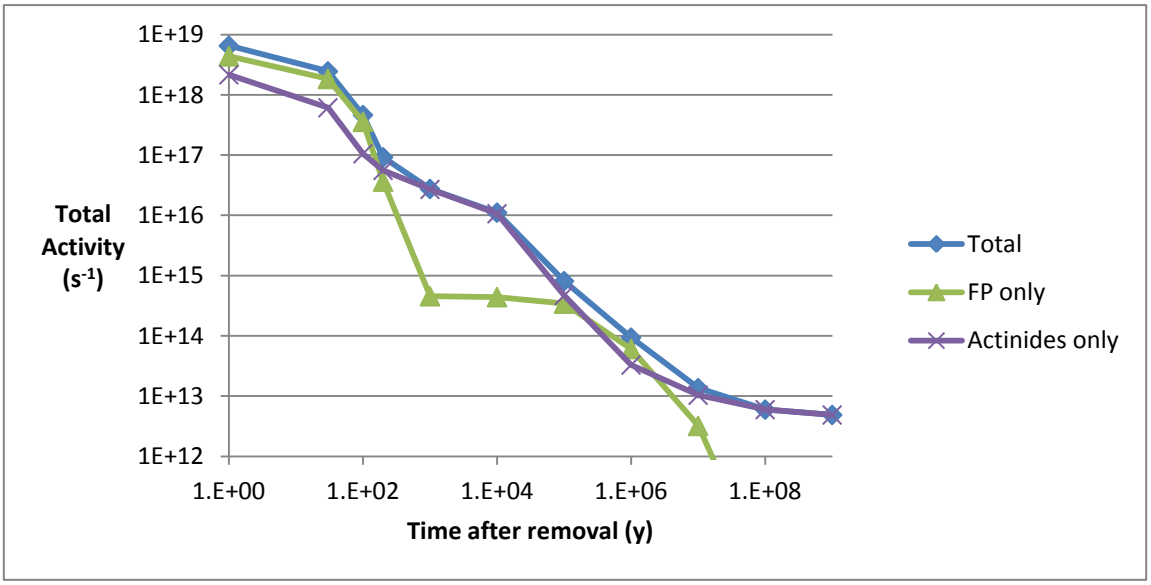

Figure 1 Total activity of spent fuel components vs. time for spent fuel from an average PWR.

1.2 Potential for transmutation as a method of disposal

Due to the long lasting hazardous nature of nuclear waste, transmutation into shorter lived and stable nuclides is a potentially attractive method of disposal. Actinides can be transmuted through fission either in fast spectrum critical reactors or in accelerator driven systems. [2] [3] Fissioning the actinides will create more fission products, while leaving the fission products from the original fuel to deal with as well. If actinides are being transmuted efficiently, the fission products will be the major source of radioactivity in the resulting waste.

Fission products cannot fission, as they are too small, but they can undergo other nuclear interactions that will change their nuclear structure to transmute them into something less problematic. As there are so few possible long lived nuclides in the region that the fission products are in, essentially any interaction will result in a stable or much shorter lived product. The shortest lived and most active LLFP is technetium-99, which can absorb a neutron to form a stable ruthenium nucleus, thus removing the radionuclide from the waste [4]. Neutrons for transmuting technetium can either be produced from fission in a reactor, or from spallation and other interactions in an accelerator based system. Systems have been designed to transmute LLFP's in reactors [5][6][7], fusion devices, [8], accelerator driven subcritical systems, [9] [10] This report aims to analyze transmutation of LLFP's in an accelerator driven system without any fissioning material present, as in [11], removing many of the safety concerns present in fissioning systems.

1.3 Thesis objectives

The objectives of this thesis are (1) to evaluate potential methods for transmuting fission product inventories in spent nuclear fuel compositions using a non fissioning accelerator based system and (2) assessing the impacts that this would have on waste inventories, while (3) optimizing the systems suitable for these methods. The ^{99}Tc transmutation target design is intended to optimize the transmutation efficiency, by increasing spallation neutron creation and decreasing leakage to increase the number of Tc atoms transmuted per unit of energy input into the accelerator. The MYRRHA linear

accelerator was used to obtain reference values for the accelerator efficiency and beam geometry. [12]

The parameters being investigated are:

- Target nuclide selection: ^{99}Tc, or ^{129}I and ^{135}Cs
- Incident proton beam energy
- Target material composition: addition of spallation and scattering materials
- Target geometry: cylinder with central beam hole

The performance of the system will be evaluated using computed values of:

- Transmutation efficiency: target nuclei destroyed per unit of energy input
- Rate of ^{99}Tc destruction: effective halflife in target
- Amount of ^{99}Tc required to make target
- Impact of transmutation scheme on waste management

2. NEUTRON INTERACTION ANALYSIS OF LLFP'S

Fission product transmutation is an important possibility for the reduction of long term risks of the storage of spent nuclear fuel. Seven long lived fission products exist: ^{99}Tc, ^{126}Sn, ^{79}Se, ^{93}Zr, ^{135}Cs, ^{107}Pd, and ^{129}I. Of particular interest are ^{99}Tc, ^{129}I and ^{135}Cs, which all have relatively large yields from fission and ^{126}Sn which has a particularly dangerous decay chain. The other nuclides are of lesser importance and will be discussed in less detail here. The fission yields of the four more important LLFP's can be seen in Table 1. [13]

Table 1 Accumulated yields for thermal and fast fissions of different fuels.

Yield for	I-129 (%)		Yield for	Tc-99 (%)	
Neutron	.0253 eV	1 MeV	Neutron	.0253 eV	1 MeV
^{235}U	0.718	0.8273	^{235}U	6.11	5.714
^{238}U	0	1	^{238}U	0	6.196
^{239}Pu	1.39	1.52	^{239}Pu	6.14	5.984
Yield for	Cs-135 (%)		Yield for	Sn-126 (%)	
Neutron	.0253 eV	1 MeV	Neutron	.0253 eV	1 MeV
^{235}U	6.533	6.571	^{235}U	0.055	0.138
^{238}U	0	6.811	^{238}U	0	0.063
^{239}Pu	7.615	7.447	^{239}Pu	0.266	0.305

^{99}Tc is the largest contributor among fission products to long term radioactivity. It decays by a nearly pure beta emmission to the stable nuclide ruthenium-99 with a 211000 year half life and a total decay energy of 0.294 MeV. With a halflife of over two hundred thousand years, ^{99}Tc survives for a very long time but still decays fast enough to have a substantial activity when compared to most naturally occuring radionuclides. The

two other long lived technetium isotopes are ^{97}Tc and ^{98}Tc. Isotopic separation or contamination of other technitium isotopes in spent fuel is not a concern due to the extremely low accumulated yields (1e-12) for these isotopes. The cross sections for neutron absorption in ^{99}Tc can be seen in Figure 2.

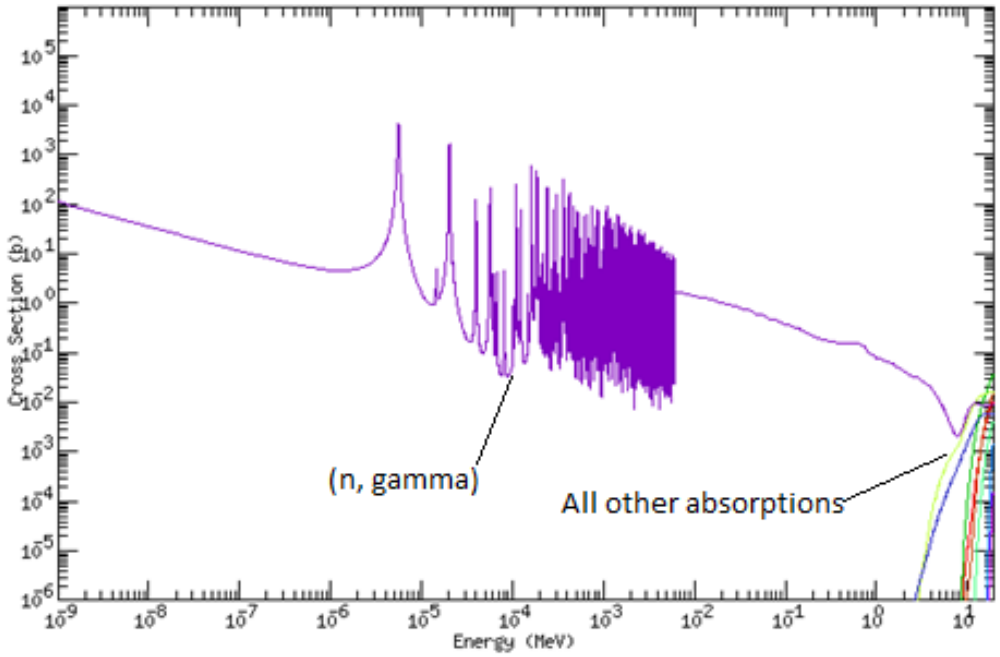

Figure 2: Neutron absorption cross sections of interest for ^{99}Tc

Radiative capture dominates below 10MeV. Radiative capture produces Tc-100 with a 15.8s half-life, decaying to the stable isotope Ru-100. The (n, 2n) and (n, 3n) reactions are not beneficial, because they produce longer lived Tc isotopes, but the number of these interactions is small compared to the radiative captures.

The cross section of ^{99}Tc is large enough to be feasible while the chemical properties of Tc allow for separation from other elements of spent fuel.

^{129}I is the longest lived radioactive fission product, with a half-life of $1.57*10^{7}$ years. It decays to ^{129}Xe by emitting a 0.154 MeV beta and a .04 MeV gamma, with energies large enough that they cannot be ignored. Iodine is a halide and can form covalent bonds readily and will react with many other substances. This could lead to accelerated dispersion into the biosphere if the iodine containing compounds are exposed. The fact that iodine is concentrated in the thyroid gland of humans is also a cause for some concern; the dose rate is small, but over time people with higher ^{129}I concentrations in their diet could suffer from radiation related problems. Cross sections for ^{129}I can be seen in Figure 3 .

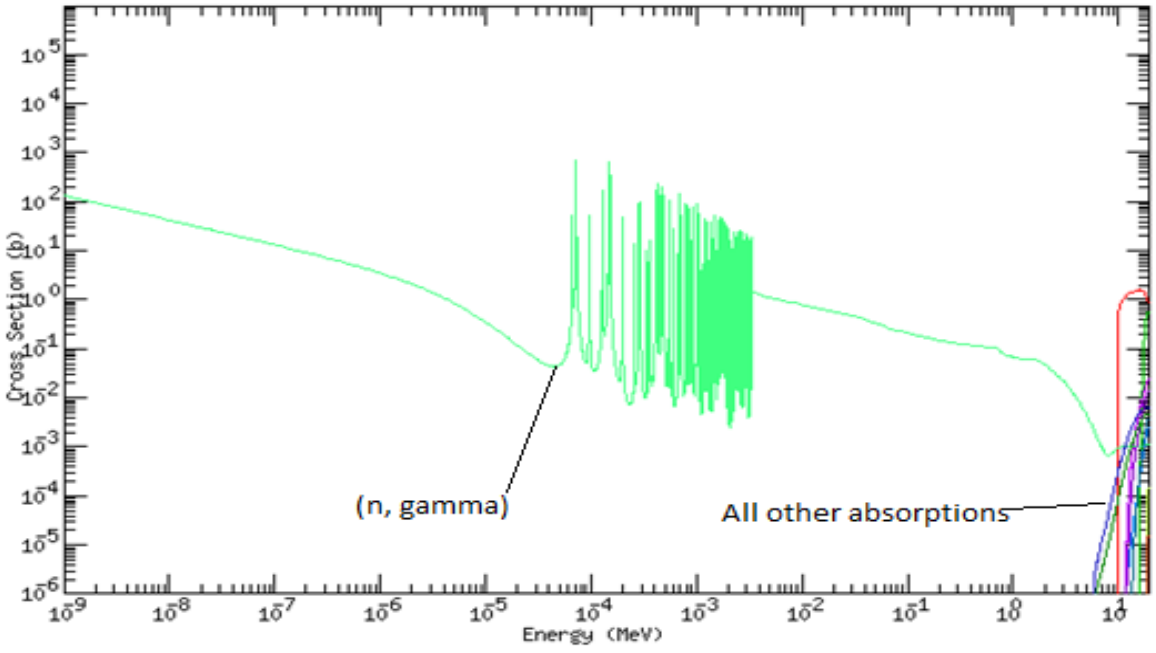

Figure 3: Neutron absorption cross sections for ^{129}I

Radiative capture is the primary mechanism for transmutation below 10MeV. This produces ^{130}I, with a 12.36h half-life, producing the stable isotope Xe-130. The thermal cross section is large enough that iodine-129 transmutation is feasible. An additional concern with the transmutation of ^{129}I is the presence of the stable ^{127}I isotope in spent fuel, and the radioactive ^{131}I isotope. ^{131}I is dangerous in events involving containment failures in operating reactors, but is relatively short lived, and will have effectively all decayed before any separation process is done on the spent fuel. ^{127}I has a fission yield that is approximately one fifth the yield for ^{129}I, and the cross section for thermal capture is approximately one eighth the size of the ^{129}I cross section. This results in a neutron loss of about one neutron to ^{127}I for every 40 absorptions in ^{129}I. The ^{128}I produced is short lived, so poisoning from the lack of isotopic separation of iodine isotopes found in spent fuel is therefore not a major concern.

^{135}Cs is another fission product of note. With a 2.3 million year half-life it undergoes a 270 keV beta decay to the stable nuclide ^{135}Ba; Cs is primarily a concern for internal dosage, due to the lack of a prevalent gamma. As an alkali metal, cesium almost exclusively occurs as a cation. This results in a high solubility in water and concerns about dispersion if water reaches the waste forms. Cesium-135 also has the largest accumulated yield of the 7 long lived isotopes, being created in the decay chains of 6.9% of thermal fissions. The separation, reprocessing and transmutation of ^{135}Cs is complicated by the almost equally abundant supply of ^{137}Cs in spent fuel. ^{137}Cs is a potent beta and gamma emitter with a 30 year half-life and a very small absorption cross section. The separation of the two isotopes would require an enrichment process that

would be dangerous due to the high radioactivity of the ^{137}Cs. The only practical way to attempt to transmute ^{135}Cs would be to wait 100 years or more, or to put it in the reactor with the 137. The cross sections for ^{135}Cs can be seen in Figure 4.

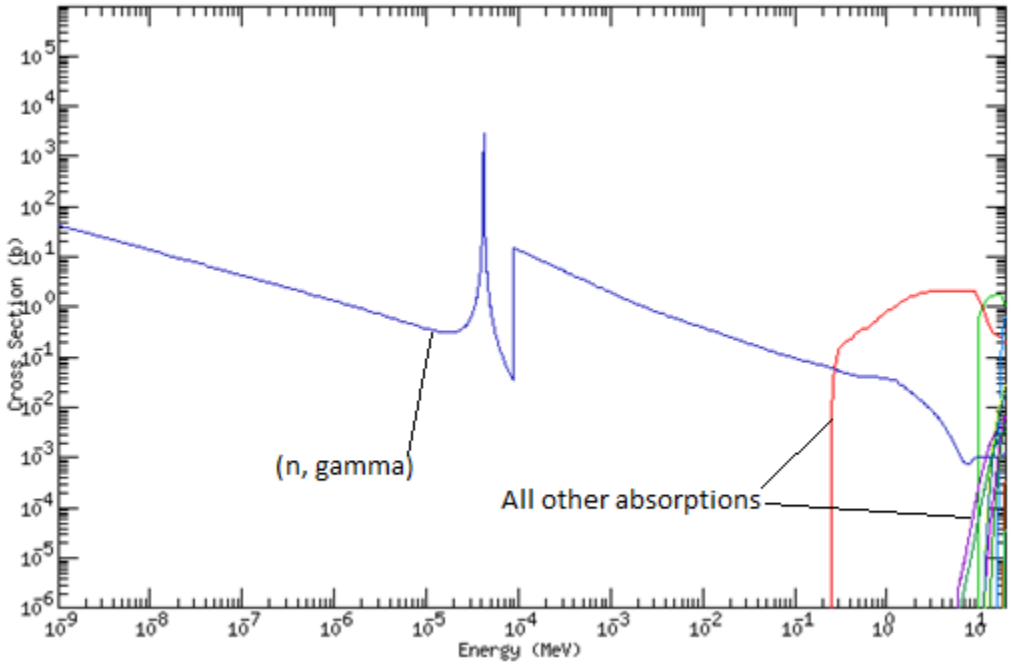

Figure 4: Cross sections for ^{135}Cs

Radiative capture is the main mechanism for transmutation. This produces Cs-136 with a 13.6 day half-life which in turn produces the stable isotope Ba-136. The (n, n) inelastic scatter that is present above 0.25 MeV is not useful for transmutation because the metastable Cs-135 isotope does not decay into another nuclide.

^{126}Sn is a somewhat concerning fission produce because of its decay chain. ^{126}Sn beta decays to ^{126}Sb with an approximately 230,000 year half life and a decay energy of 380 keV. ^{126}Sb in turn decays by emitting a beta with an energy ranging from 0.196 to 1.894 MeV, and gammas with energies up to 1.476 MeV. The total decay energy is 3.67 MeV. The higher energy gammas are quite penetrating, making tin the largest mentioned external irradiation hazard. The yield of ^{126}Sn from thermal fissions in ^{235}U is only 0.055%. This is because the atomic mass number 126 is close to a 50/50 split, which is uncommon for thermal fissions. Fast fissions in heavier actinides can increase the yield to .26% for fast reactor neutrons in ^{239}Pu, and as high as 2% in fissions caused by 14 MeV neutrons produced from D-T fusion. The low yield from most reactor fuels leads to a low total heat loading from ^{126}Sn when compared to ^{99}Tc. Tin is also a fairly inert metal, so mobility in the environment is limited in any foreseeable breach of storage. Storage of ^{126}Sn therefore has an increased level of inherent safety in the element's chemical properties. The neutron cross sections for ^{126}Sn can be seen in Figure 5.

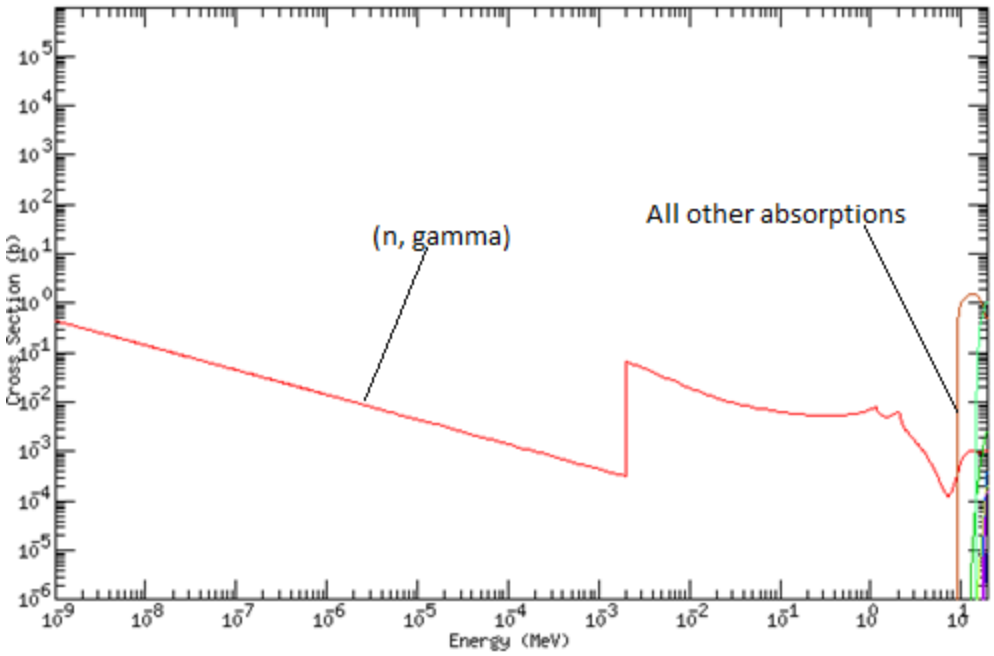

Figure 5: Cross sections for ^{126}Sn

The cross section for absorption is very small. In energies below 10 MeV, the cross sections are all less than 1 barn, primarily on the order of .01-.1 barns. The cross sections for ^{126}Sn are too small to allow for efficient transmutation.

All radiative capture cross sections cam be seen in Figure 6, with ^{99}Tc is shown in red, ^{129}I in green, ^{135}Cs in blue and ^{126}Sn in violet. The thermal cross sections are on the order of 20-100 barns for Tc and I, about 1-30 b for ^{135}Cs, and less than 0.5 barns for Sn-136. The resonance absorption region has the largest cross sections for all three reasonably fissionable isotopes, though the lowest thermal cross sections are nearly as large when averaged. The iodine-129 and technetium-99 are both more readily transmutable using neutrons, while the cesium-135 and tin-126 are not.

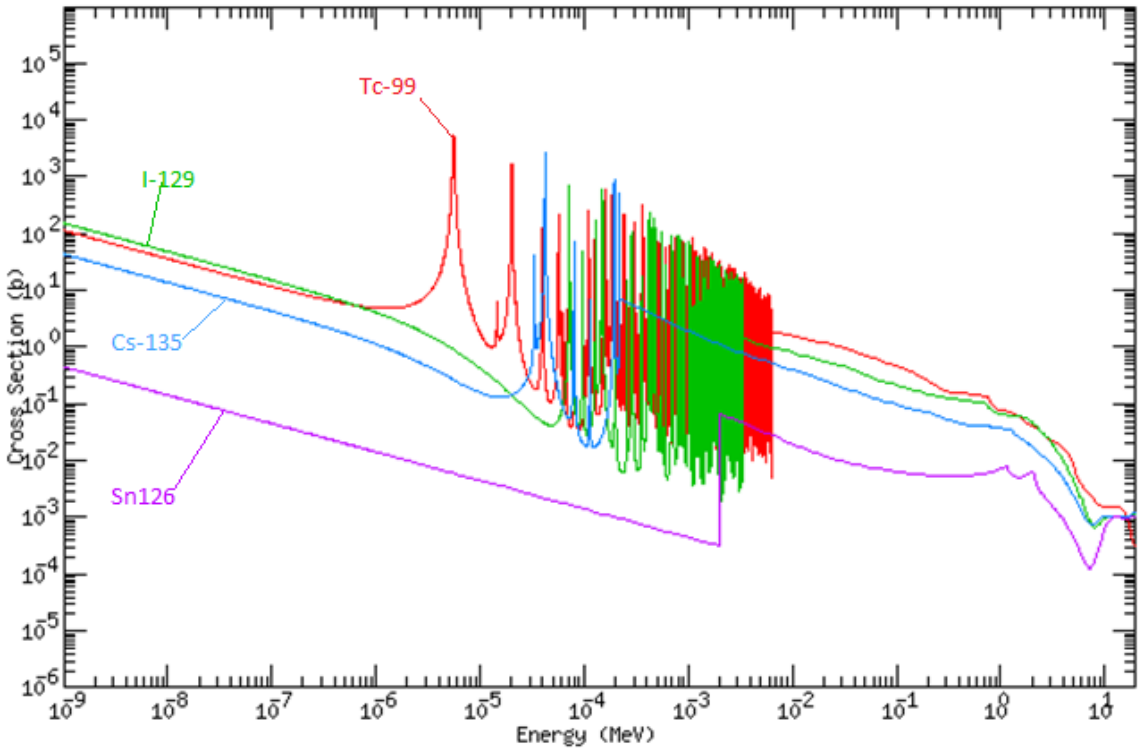

Figure 6: Radiative capture cross sections for the four primary long lived fission products

^{99}Tc is a viable candidate for neutron based transmutation due to its appreciable capture cross section and the feasibility of chemical separation for reprocessing. Epithermal neutrons would be ideal for ^{99}Tc transmutation, due to its large resonances. A system in which there is a high epithermal neutron flux is present, such as a blanket region of a fast reactor, or a specifically designed system would provide the optimal ^{99}Tc transmutation rates.

^{129}I is another potential candidate for transmutation, due to its large cross section and its chemical properties, which allow for easier separation. The production of a mechanically and chemically stable target form for the irradiation of iodine is a minor concern, as is the presence of ^{127}I in the target. The most useful neutron cross section for ^{129}I transmutation is thermal capture, so thermal neutrons have the greatest potential for efficient ^{129}I transmutation.

^{135}Cs is not particularly feasible to transmute. The smaller cross section and hazards involved in separating or handling the ^{137}Cs found in the spent fuel make the transmutation of ^{135}Cs impractical and unsafe without significant increase in shielding.

^{126}Sn is unfortunately not at all feasible for neutron based transmutation. The cross section is far too small for any effective efforts at transmutation by neutron bombardment. The chemical stability of tin can be utilized to safely store it in a long term repository and prevent escape into the biosphere. Additionally, the neutron cross sections for ^{137}Cs, ^{90}Sr, ^{107}Pd, and ^{93}Zr are small enough that effective transmutation by neutrons is not feasible. ^{79}Se has a small yield for fission and has not been analyzed for neutron transmutation in this report.

3. CHARGED PARTICLE TRANSMUTATION ANALYSIS

3.1 Modeling approach

MCNP is used as the primary modeling tool, specifically MCNPX, the extended version of MCNP5. MCNP was chosen due to its availability, robust physics models and treatment of charged particles, and the ability of montecarlo codes to be run in analog mode. Initially, an infinite pure target was modeled, with protons at a single energy spawning within the target. The beam was assumed to be 100% efficient at converting energy into the kinetic energy of the particles, and the infinite medium creates a system in which no particles are wasted to leakage. The infinite target contains ^{135}Cs and ^{129}I and nothing else. By setting all energy cutoffs to zero for neutrons and an energy less than the energy required to overcome the coulomb barrier for protons, the system can be run in analog mode, tracking every particle until its death. This allows for easy determination of the number of transmutation, as the number of neutrons and protons lost to interactions that would transmute a nucleus is the number of transmutations occurring. MCNP tracks particle creation and loss by the creation or loss mechanism in the output file. Mechanisms resulting in transmutation include capture, (n, xn) and the other nuclear interaction group for protons and neutrons. Physics models in MCNP are used to compute the cross sections for high energy particles on the fly to determine how many interact across a specific path. The number of particles lost to interactions comes from these physics models. The transmutation efficiency is defined as the number of nuclei transmuted per MeV of incident particle energy, as seen in Equation 1:

$$\text{efficiency} \quad \frac{\text{total number of transmutations}}{\text{total energy of incoming particles}} \ (\text{Me}^{-1}). \qquad (1)$$

The inverse of the efficiency is the average amount of kinetic energy input required to transmute one target nuclide, or the energy requirement per transmutation [11]. In the infinite model, different incident particle energies for protons, deuterons and alpha particles will be run to determine energy dependence and the effectiveness of each beam.

An infinite target is simple and can provide some information about maximum efficiencies where leakage reaches zero, but any real target must be finite, as infinite objects are impossible to construct. The finite target designs all consist of a cylinder, with the particle beam incident on a flat face of the cylinder. Most designs have a cylindrical hole that penetrates partway through the radial center of the cylinder for the beam to enter. The dimensions of the target are varied for different target designs, but the same form is used throughout and can be seen in Figure 7. Goals in designing the target are to have a high transmutation efficiency by lowering leakage, a lower average nuclide lifetime in the target, and a lower target material mass requirement.

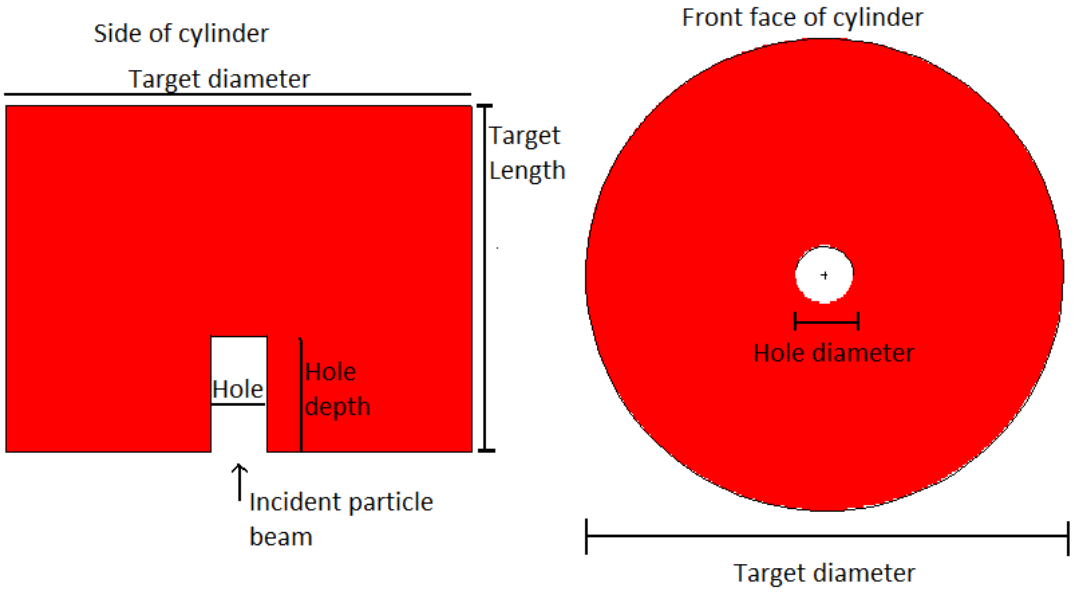

Figure 7 General target geometry

After a target geometry is selected, a comparison can be made between the use of a Cs-I target and a Tc target by testing the same geometry with each target material at the same density. The material that requires less energy to transmute each LLFP nuclide is the more efficient transmutation target, because the reduction in the radioactive inventory will be greater for the same amount of energy input into the accelerator. After finalizing the target nuclide selection, the goal is to add materials to the target that are not radioactive transmutation target nuclei. This can improve the characteristics of the target by reducing leakage or increasing spallation neutron generation. The addition of a spallation material improves neutron production, and a reflector material around the target decreases leakage to decrease the required energy per transmutation without increasing the amount of target material used. Adding other nuclei to the geometry

causes a problem in that it invalidates the previously employed method of counting transmutations. The problem with adding non target materials is that the method currently used for calculating the number of transmutations involves reading the total number of protons and neutrons lost to capture, (n, xn) or other nuclear interactions, and taking this number to be the number of target nuclei transmuted for the given number of source particles. MCNP's particle creation and loss tracker does not inherently distinguish between particle losses to different nuclei, so some particle losses to interactions would not result in transmutations. The method that has been used thus far cannot distinguish between nuclear interactions in the target nuclides and those occurring with the other materials. Another method of estimating the number of transmutations must be found.

An interaction tally could provide an estimate of the number of interactions of any specified type with technetium nuclei. An issue is that MCNP interaction tallies do not score interactions in the model cross section regime. The tabulated data for Tc-99 used in MCNP does not cover the entire range of energies involved in this system, causing a tally to ignore all of the higher energy interactions with Tc nuclides. The ENDF/B-VII.0 libraries for ^{99}Tc are only evaluated up to 20 MeV. [14] A custom tally can be input into MCNP to count the interactions with higher energy particles. Energy bins weighted by the average cross section for that bin estimate the number of interactions in each energy bin and thus the total number. An existing database, TENDL libraries produced using the TALYS code could be used for the cross section data, but the model based cross sections from TALYS differ from those used in MCNP. This

causes the loss rate of particles and the counted interaction rate to differ, and prevents the particle loss method and tally method from agreeing in a pure Tc target. To tally the interactions in a self consistent manner within MCNP, it is necessary to use cross section data based upon the physics models used in MCNP. Regardless of which cross section library's set of models better represents reality; it is beneficial to use the same physics models for both the particle transport and the tallying. A resolved resonance in the MCNP model that is not in or not as large as the resonance in the cross section data used for the tally could cause many particles to be lost to interactions without tallying an adequate amount. Discrepancies in the resonance region can result in potentially large errors in transmutation rates. [9] Also, cross sections based upon MCNP's physics models must be used to validate the tallying method by showing that it can agree with the particle loss method of counting transmutations.

A custom cross section library based upon MCNP's physics models can be produced by running simulations to measure the cross sections in MCNP. A thin target with incident particles generated with energies distributed through the bin range can be modeled to determine the average cross sections for incident particles in that energy range. The microscopic cross section in cm^{-2} can be found using:

$$\frac{n_{intr}}{nps\ N_{Tc}\ z'} \qquad (2)$$

where is the cross section, n_{intr} is the number of interactions in the MCNP output file, nps is the number of particles run, N_{Tc} is the number density of the target in atoms/cm^3 and z is the target thickness is cm.

When the average cross section for each energy bin is obtained, the total number of interactions in a more complex target can then be found using a custom weighted flux tally in the region containing target material, where each energy bin's flux is weighted using the microscopic cross section of the target material for the bin's energy range in barns. As MCNP automatically weights its tallies per source particle, the total number of interactions corresponding to a given tally is found using Equation 3, where "tally" is the tally total in the MCNP output file and V is the total volume of the region being tallied:

$$n_{intr} = \text{tally} \cdot \text{nps} \cdot V \cdot N_{Tc} \cdot 10^{-24} \text{cm}^2/\text{b}. \quad (3)$$

The total target interactions from each tally can then be added to obtain the total number of interactions occurring in the simulation. This allows for the transmutation efficiency and energy requirements to be determined in targets with other materials present.

3.2 Analysis of an infinite CsI target

The infinite target consists of ^{135}Cs and ^{129}I in a one to one ratio and nothing else. The number of particles lost to absorption or other nuclear interactions is taken to be the number of nuclei transmuted, because the target only contains nuclei that are transmutation targets. Runs with different incident particle energies provide data for the energy required per transmutation vs. the incident energy. Data collected for the infinite target can be seen in

Table 10 in appendix B. The numbers of proton and neutron interactions are obtained from the MCNPX output file by finding the number of protons and neutrons lost to any interaction. A plot showing the relative portion of transmutations caused by protons and neutrons can be seen in Figure 8. The number of transmutations caused by neutron interactions is far greater than the number of proton interactions, increasingly so as the incident energy and spallation increases.

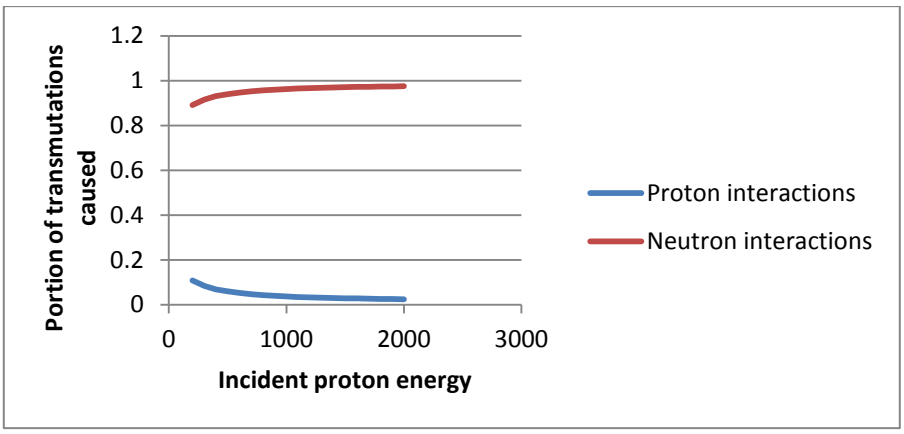

Figure 8 Portion of transmutations caused by interactions with a given particle vs. incident proton energy from the accelerator

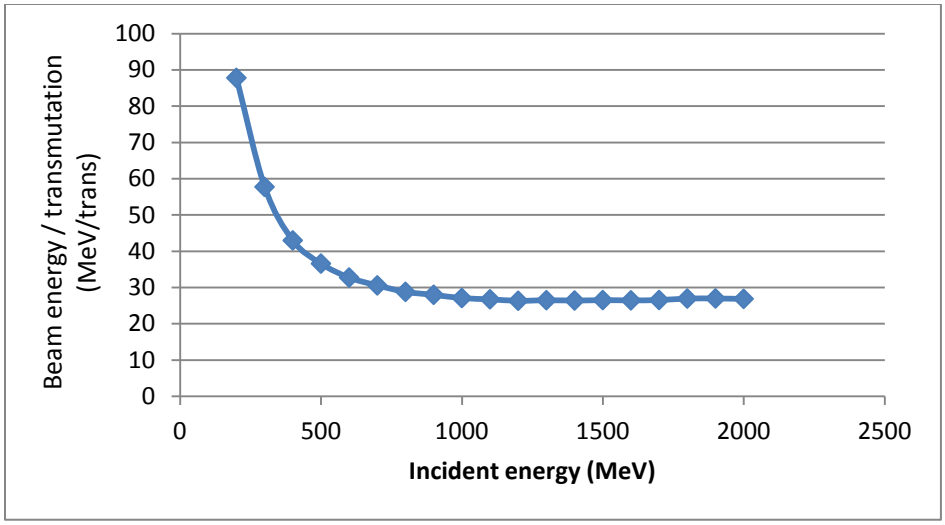

Figure 9 Plot of the energy per transmutation vs. the incident proton energy for the infinite pure target

A plot of the energy required per transmutation in the infinite target vs. energy can be seen in Figure 9. Using protons, the total incident particle energy required per transmutation asymptotically approaches a minimum of approximately 26.5 MeV/transmutation. The beam efficiency decreases with particle energy and the size of the target required for minimal leakage increases with beam energy, so a lower energy is desirable. 800-1000 MeV seems to be an optimal energy range, as the infinite target improvements of increasing it further are small.

The use of other charged particles can be considered to improve the transmutation efficiency. The results for protons, deuterons and alphas are shown in Figure 10 and in Table 11 in appendix B for comparison.

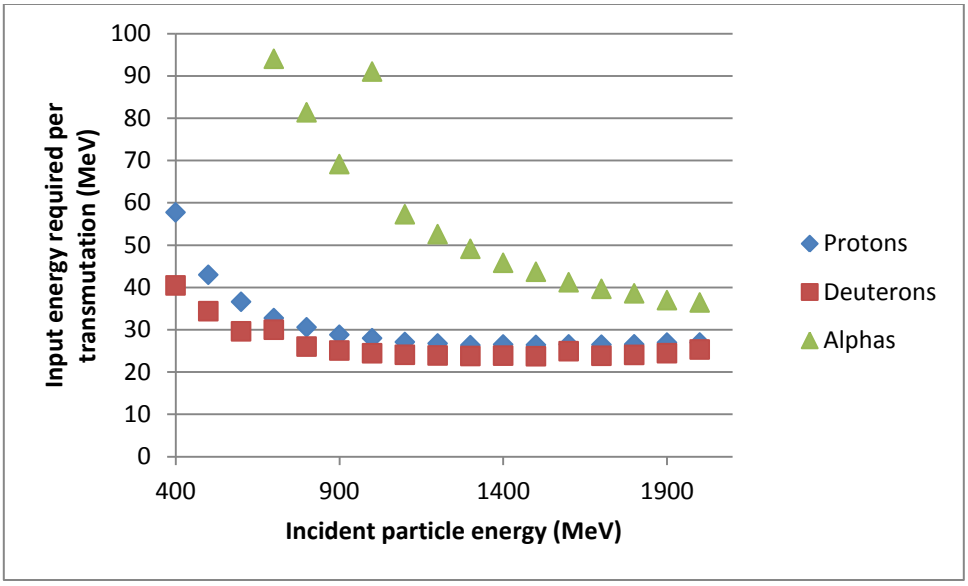

Figure 10 Energy required per transmutation vs. incident particle energy for protons, deuterons and alpha particles.

Under the assumptions that the accelerator has the same efficiency for all incident particle types, and that the particles to be accelerated can be obtained without additional energy input, deuterons will transmute the fission products with slightly less energy input. This would suggest that deuterons could be a superior choice to protons. Alpha particles transmute far less, due to the increased rate of columbic slowing caused by the doubled nuclear charge. The higher point in the alpha plot at 1000 MeV appears to be an outlier with little physical significance, and will be ignored as alphas are already clearly not the particle of choice for transmuting LLFP's.

Proton beams are far more common than deuteron accelerators, and the improvement of using deuterons instead of protons is not overwhelming, so proton beams will be used for the rest of the models.

3.3 Modeling of a target geometry in MCNPX

To model the effects of leakage and the efficiency of different target geometries, a model of a target and beam was made using MCNPX. The beam was approximated to be perfectly monodirectional and infinitesimally thin. The monodirectionality is a fair approximation due to the focused nature of particle beams, and the reference Myrrha accelerator has a relatively small beam diameter of 10 cm, so little accuracy is lost by modeling a point source. A cylindrical target was initially used, with modifications made to hollow out a section in the center on the target face to cause backscatters to be less likely to leak. The model of the first target can be seen in Figure 11. Target 1 was 150 cm long and had a radius of 100 cm. This target would contain approximately 23500 kg total of Cs and I, which is comparable to the total mass of Cs-135 and 90% I-129 in all of the spent fuel in the US. [1] The proton and deuteron data can be seen in Table 2.

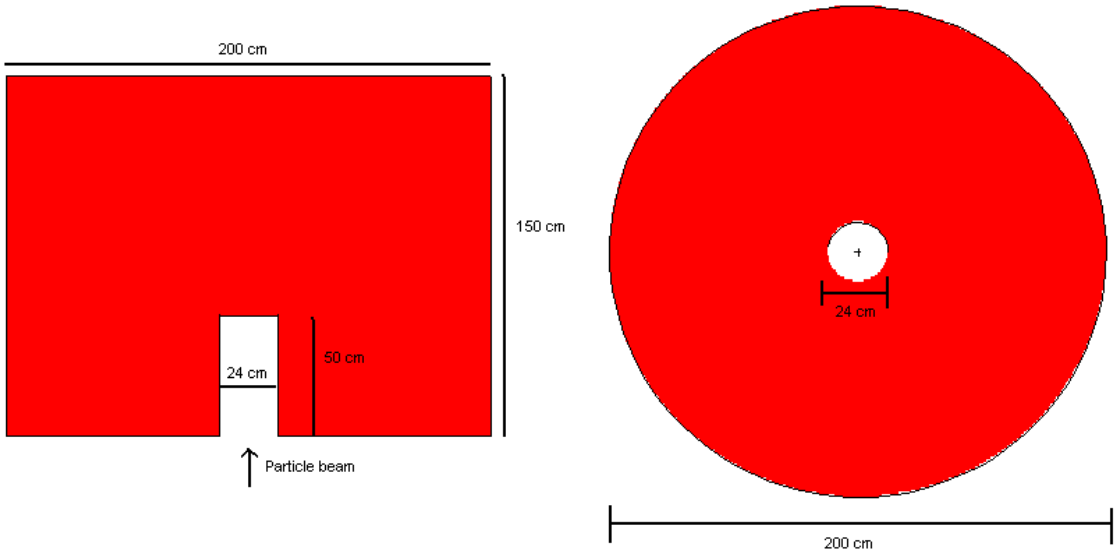

Figure 11 Diagram of target 1

Table 2 Energy required per transmutation using the large solid Cs-I target 1.

Target 1	protons		deuterons	
Incident Energy (MeV)	Total interactions	E/trans (MeV)	Total interactions	E/trans (MeV)
500	83357	59.9829	94385	52.974
600	113221	52.9937	126247	47.525
700	141029	49.6351	153409	45.629
800	166063	48.1744	186567	42.880
900	187844	47.9120	213673	42.120
1000	208910	47.8675	241384	41.428
1100	230560	47.7099	266858	41.220
1200	249520	48.0923	288528	41.590

Moving from an infinite medium to a very large though finite pure target has nearly doubled the amount of energy required to transmute each nuclide a pure CsI target. Target 1 is too large to fabricate or deal with in a real scenario, so smaller targets must be used. Target 2 is a second pure target, with an outer radius of 30 cm, a length of 50 cm, and a beam hole that is 12 cm in radius and 20 cm deep, similar in design to target 1. This particle has a total Cs and I mass of 661 Kg. The smaller target is much less efficient due to the increased leakage loss of both neutrons and incident protons, as seen in Table 3. Additionally, the smaller target has an efficiency that decreases with incident energy, due to the preferential leakage of higher energy particles.

Table 3 Energy required per transmutation using the smaller target 2

Incident Energy (MeV)	Total interactions	E/trans (MeV)
500	19931	250.8654859
600	23169	258.9667228
700	25547	274.0047755
800	28292	282.7654461
900	31314	287.4113815
1000	33012	302.9201502
1100	35187	312.6154546
1200	37482	320.1536738

Alterations to this geometry were made that involved doubling the total volume by either doubling the length in target 3 or the cross sectional area in target 4. Additionally, target 2 and 3 were altered to remove or greatly reduce the size of the beam hole and tested again, to determine whether the additional effective length outweigh the backscatter capturing effects of the beam hole. The effective length is the distance from the point the beam hits to the back vacuum boundary, and is essentially the total length in which the particles may be caught. The modified targets are essentially cylinders with the same diameters and lengths. The data from these geometries is in Table 4. The improvement in transmutation efficiency obtained by increasing the diameter is small, as the values for target 4 are only slightly smaller than for target 2. Increasing the length of the target from 50 cm to 100 cm and effective length from 30 cm to 80 cm greatly increases the efficiency as can be seen from the large difference in the energies in target 3 and target 2. The removal of the hole increased the efficiency in

target 2 due to the increased effective target length reducing leakage from the incident charged particles and the heavily forward biased spallation neutrons, but in target 3, the removal of the hole actually decreased the efficiency at energies below 900 MeV, due to the loss of the backwards scattering particles. This energy dependence can be seen in the plot of the efficiencies in Figure 12 below and suggests that the optimal effective length of the target for which a large portion of the protons and spallation neutrons are utilized is positively correlated with the incident energy and that 80 cm effective length is not long enough for most of the energies in this range. It also shows the benefit of having the beam hole to catch the neutrons that end up travelling backwards, given that the effective target length is sufficient for the incident energies used. Of the trials run here, the 800 MeV beam on the long, thin target 3 with a hole was the most efficient suggesting that a greater target length is more beneficial than a greater width. Thus an optimal geometry with limited target material would be longer than those tested here, though not necessarily wider, and contain a beam hole that is at an optimized depth for which the backscattering particles are caught and the forward biased momentum of the particles has enough distance to be captured as well.

Table 4 Energy per transmutation at different incident proton energies for different target designs

Incident Energy (MeV)	Target 2		Target 3		Target 4
	50 cm h	30 cm R	100 cm H	30 cm R	50 cm H 42.4 cm R
	20x12 hole	2x12 hole	20x12 hole	No hole	20x12 hole
500	250.8655	194.5677	162.8399	169.641	217.1929977
600	258.9667	187.8169	148.7948	153.4291	221.5657312
700	274.0048	193.9972	142.7057	145.7058	233.3877905
800	282.7654	197.2484	139.8748	141.4352	238.5282805
900	287.4114	201.8028	140.9509	140.0299	247.2255796
1000	302.9202	209.1613	144.3231	140.4376	256.344527
1100	312.6155	212.8648	144.7311	139.8939	259.97353
1200	320.1537	215.2505	145.4263	140.8385	270.7092583

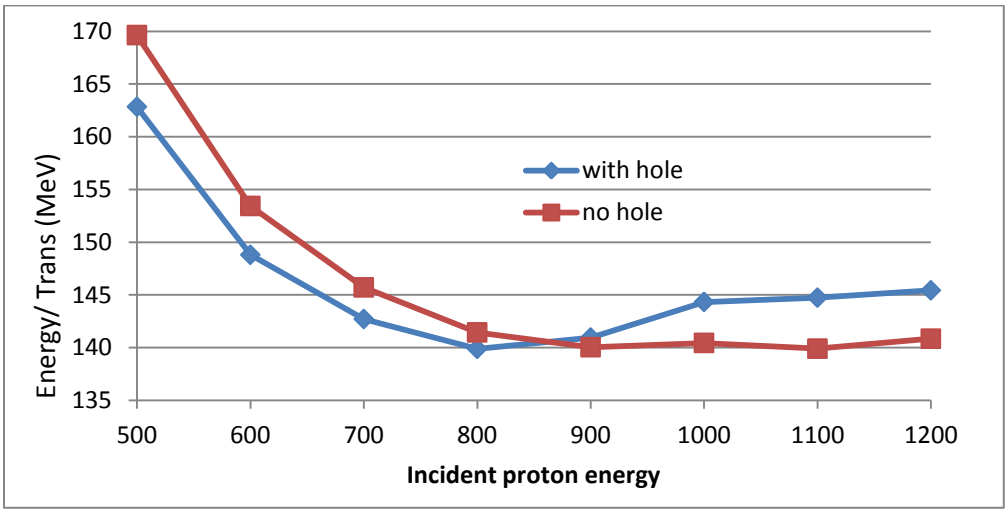

Figure 12 The energy required per transmutation in target 3 with and without the beam hole.

The largest contributing factor to the high energy requirements for transmutation of the cesium and iodine nuclides is the leakage of neutrons produced by spallation. The addition of a reflector could improve the efficiency by reducing leakage, as would increasing the cross section of the target nuclides. As the cross sections for a nuclide are inherent to its nuclear structure, the only way to alter them is by using a different nuclide. technitium-99 has a larger cross section than either cesium-135 or iodine-129 for most of the resonance region and at higher energies. As the neutrons produced in the spallation reactions are at very high energies, ^{99}Tc would be a more feasibly transmuted target.

3.4 Modeling a finite ^{99}Tc target

^{99}Tc is more easily transmutable in an accelerator driven system such as the one being modeled here due to its larger resonance and high energy absorption cross sections. The larger absorption cross section causes more neutrons to be absorbed to transmute target nuclei, and less to leak out of the system. To compare the efficiency of transmuting ^{99}Tc to transmuting a combination of ^{135}Cs and ^{129}I, one of the targets modeled for transmuting CsI was modeled with ^{99}Tc as the target material. The density of Tc was set to 5 g/cm^3 to be the same as the CsI target for a better comparison. Target 3 with the 20 cm beam entrance hole was used for the comparison models. The results can be seen in Table 5.

Table 5 Energy required per transmutation in CsI and Tc targets

Incident Energy (MeV)	Energy per transmutation (MeV)	
	CsI target 3 with hole	Tc Target 3 with hole
500	162.3851	99.82232
600	147.0552	91.45784
700	142.343	87.69512
800	138.7011	85.30876
900	138.3998	84.35022
1000	141.9829	84.67974
1100	142.9463	85.54453
1200	144.882	86.41362

The input energy required per transmutation in the technetium target is approximately 40% less than in the CsI target. This means that 1.6 times as many Tc nuclides would be destroyed with the same target geometry and mass of target material present. ^{99}Tc will therefore be used as the target nuclide for further modeling.

3.5 Cross section bin generation in MCNPX

In order to tally the interactions occurring between technetium nuclei and particles with energies above MCNP's tabulated cross section data, cross section bins must be generated. To measure the average cross section within a bin, a short and very thin cylindrical technetium target was modeled with a monodirectional point source of particles axially incident on the face of the cylinder. A separate MCNP deck was run for each energy bin, with particles being born with an energy randomly selected from the energy bin. The target was small enough that attenuation and scattering buildup are negligible. If these assumptions hold, the cross section is given by Equation 2. A smaller

target requires more particles to be run to attain good statistics, so to reduce computation time, a larger target that is still small enough for minimal attenuation is optimal. Different sizes of targets are used at different energies, so that enough particles interact without reaching the level where attenuation and energy loss effects must be accounted for. The goal in selecting the target thickness is that less than 10% but more than 0.1% of the particles incident on the cross section measuring target interact in the target. Additionally, to cut out interactions from particles that are at energies outside of the bin range, the energy cutoff for the particles of interest in a specific run was set to the bottom of the bin range for which the cross sections are being measured. There was difficulty accurately modeling the resonance absorption region using finite custom cross section bins, due to the fine details of the resonance capture region. The error in resonance resolution can be seen in Figure 13. The issue is that accurately resolving resonances in a custom generated library using the same method used for the high energy portion of the library would require a prohibitively large number of bins to avoid large errors between the number of particles lost to interactions in technetium and the number of interactions tallied. A custom tally therefore cannot be used to tally the captures in the resolved resonance region.

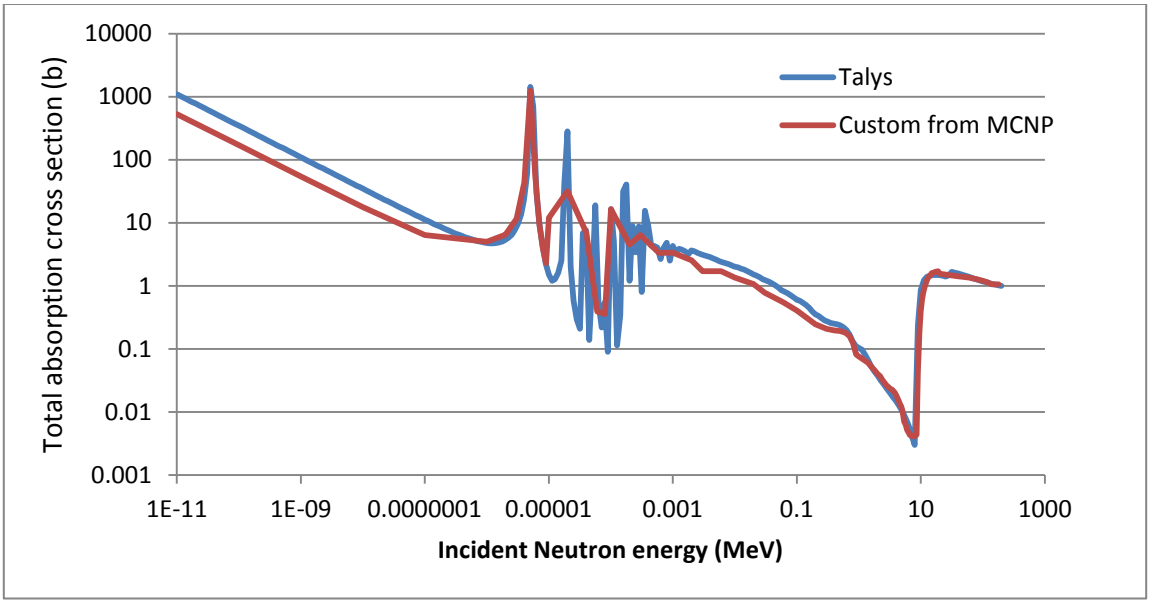

Figure 13 Total neutron absorption cross section vs. energy in custom built library and using TALYS library.

MCNP's capture tally can be used to tally the lower energy neutron captures, which fall off to near zero before the energy exceeds the tally range. A custom made tally can be used for all other nonscattering nuclear interactions, which begin to occur above about 9.1 MeV. The proton interactions are all tallied using custom bins, starting at 1 MeV, as protons with less than a few MeV cannot effectively overcome the coulomb barrier to interact directly with nuclei without undergoing very improbable quantum tunneling. Thus, the low energy captures in the resolved resonance other interactions are successfully tallied using computed interaction cross sections, leaving very few particle interactions uncounted. Iterations of energy bin and input deck designs were performed to obtain the final cross section bins and data used. The final data used in the transmutation analysis can be found in Appendix A. To validate the data

collected, it was used to estimate the number of transmutations in a pure ^{99}Tc target, so that two methods could be compared in the same system. Target 3 with pure technetium-99 at a density of 11 g/cm^3, incident proton energies of 600 MeV and 1200 MeV and 10000 source particles gives total interaction measurements of 111067 and 278427 when using the tallies. The totals obtained by counting the number of particles lost to each interaction type are 111997 and 279428. The tally method yields results that are 0.81% and 0.36% lower in these two trials. Errors less than 1% are deemed to be acceptable, as they are comparable to the uncertainties of the Monte Carlo simulations used to obtain the data. The close agreement of the two methods in the pure target therefore validates the use of the tallies in more complex targets containing multiple different nuclides.

3.6 Analysis of a target containing multiple materials

With the cross section libraries and tally method developed and validated, work on modeling targets with additional materials can begin. The goal is to reduce the required amount of technetium in the target while maintaining or decreasing the energy required per transmutation. With a fixed beam power, this will decrease the effective halflife of the technetium in the system, allowing it to be depleted more quickly.

The major addition is a target that is interspersed with the technetium to act as a spallation target and internal reflector, allowing the technetium to be spread out to capture more neutrons. An ideal material for this purpose would have a high atomic mass to increase spallation neutron production and a very low neutron absorption cross section to reduce the parasitic neutron absorption in non target material. The use of a

fissionable or fissile material is being ruled out at this stage, to avoid the complications of fissioning in the system, such as the high heat production. Additionally, a material that is relatively common and cheap would be ideal. With these constraints, lead was selected to add to the target. Lead has an average atomic mass of 207, and its neutron absorption cross sections are relatively small, as seen in Figure 14. The cross section for capture in ^{99}Tc is orders of magnitude larger than that of any stable lead isotope through the lower energy regimes and most of the resonance region, where the majority of neutron absorptions are occurring.

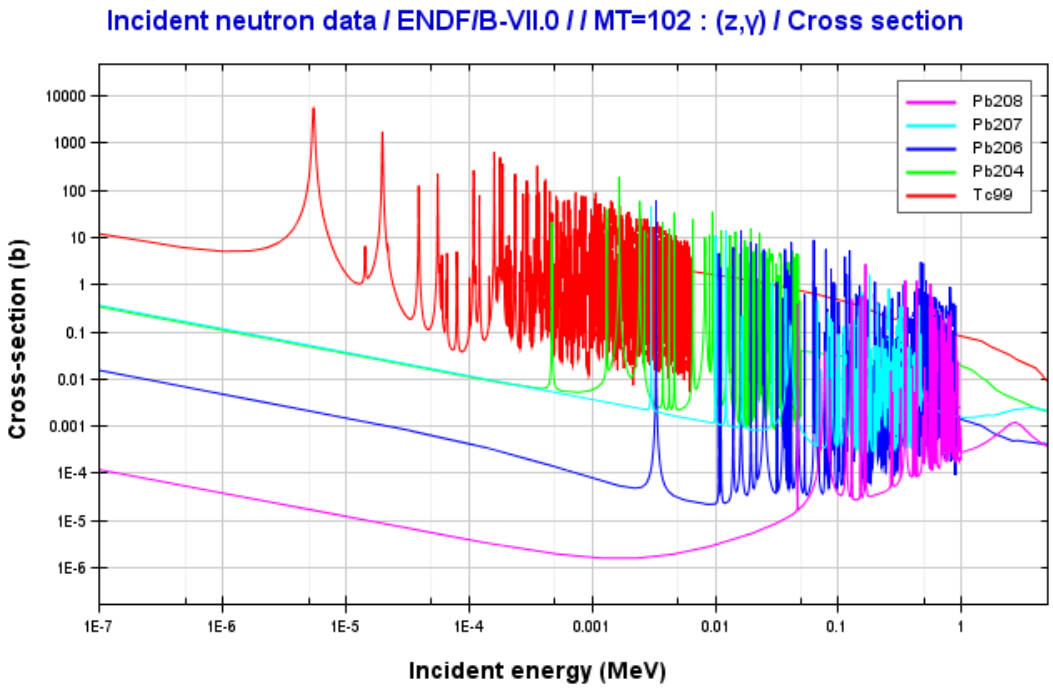

Figure 14 Capture cross sections for Tc-99 and all stable lead isotopes

A reflector around the target could improve the transmutation efficiency by reflecting some of the escaping neutrons back into the target. Graphite was chosen as a reflector material, because it has a low absorption cross section, effectively reflects neutrons of a wide range of energies, and is quite cheap to obtain. In modeling the new targets, the target region contains a homogenous mixture of ^{99}Tc and natural lead. While the Tc and lead may be separate in a real system, the neutron diffusion length is large in the target, and treating it as homogenous saves a lot of modeling and computation time. Also, the % technetium content can be easily varied by changing the material card. The target geometry used is similar. The reflector is added as a shell around the cylindrical target, with the same hole for the beam to enter through. The design for target 4 can be seen in Figure 15.

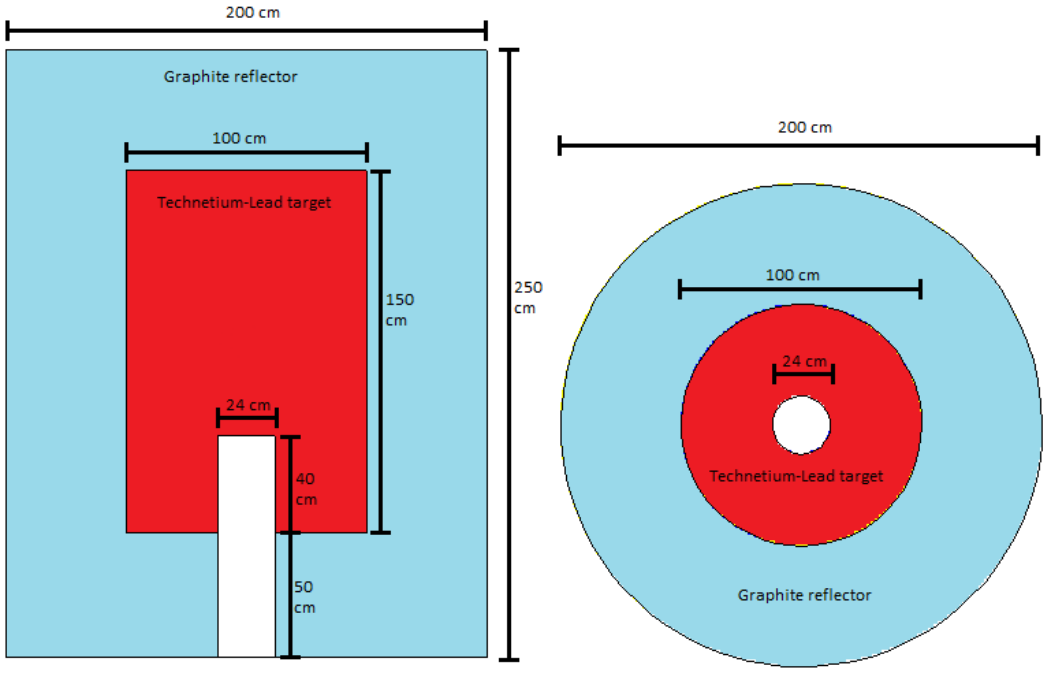

Figure 15 Target 4 design with lengths

3.7 Multi-material target results and optimization

The optimization goal for the target design is to maintain a low energy requirement per transmutation while also decreasing the amount of technetium present in the target. This will yield a system that is efficient and easier to synthesize due to the reduced target material requirement. It will also shorten the average technetium nuclide's lifetime in the target. To calculate the transmutation rate and thus the initial technetium halflife in the target, the Myrrha 600MeV beam accelerator was used as a reference model. The Myrrha accelerator has a continuous beam power of 2.4 MW, corresponding to approximately 2.5 x 10^{16} protons per second. The beam power in this model is set to 2.4MW, with a proton production rate corresponding to the number of protons at the incident energy that this will supply. It was assumed that the accelerator efficiency would be similar to the Myrrha system at 50%, putting the total power requirement at 4.8 MW. The estimated number of transmutations per technetium 99 atom produced if the accelerator was powered by thermal reactor with 30% efficiency is also computed using the beam energy requirements and the yield for ^{99}Tc production from thermal fission in uranium 235, 6.1%.

Target 4 has a total technetium-lead volume of 1159967 cm^3. With the target density set to 11 g/cm^3, and a technetium content of 10% by atom, the total mass of technetium-99 in the target is 644 kg. This is in comparison to the total mass of ^{99}Tc produced in a PWR each year, 33.1kg, or 663 kg over 20 years. [1] The results of the analysis of this target with 10% Tc content and varying incident beam energies can be seen below in Table 6.

Table 6 Results for target 4 with 10% Tc content, totaling 644 kg of Tc

Incident Energy (MeV)	Energy per Transmutation (MeV)	Transmutation rate (atoms/s)	Initial halflife (years)	Transmutations per Tc99 atom produced
700	49.60794	3.02E+17	285.0314	9.897576
750	48.46823	3.09E+17	278.483	10.13031
800	46.88648	3.2E+17	269.3947	10.47207
850	46.10062	3.25E+17	264.8794	10.65058
900	45.03281	3.33E+17	258.7441	10.90313
950	44.347	3.38E+17	254.8037	11.07174
1000	43.62432	3.43E+17	250.6514	11.25515
1050	43.60217	3.44E+17	250.5241	11.26087
1100	43.02526	3.48E+17	247.2094	11.41186
1150	43.00407	3.48E+17	247.0876	11.41749
1200	42.70547	3.51E+17	245.372	11.49732

The total amount of technetium required in this simulation was fairly large, so the technetium content in the geometry was reduced to 5% and then to 2% with the other factors remaining the same. The results for the new simulations can be seen in Table 7 and Table 8 below.

Table 7 Results for target 4 with 5% Tc content, totaling 313 kg of Tc

Incident Energy (MeV)	Energy Per Transmutation (MeV)	Transmutation rate (atoms/s)	Initial halflife (years)	Transmutations per Tc99 atom produced
700	57.86699	2.59E+17	161.7897	8.484947
750	56.38125	2.66E+17	157.6357	8.708539
800	54.88782	2.73E+17	153.4603	8.945488
850	53.07272	2.82E+17	148.3854	9.251427
900	52.07883	2.88E+17	145.6066	9.427985
950	51.63093	2.9E+17	144.3544	9.509772
1000	50.66335	2.96E+17	141.6491	9.691391
1050	50.53846	2.96E+17	141.2999	9.715341
1100	49.78265	3.01E+17	139.1868	9.862841
1150	49.90479	3E+17	139.5283	9.838702
1200	49.51769	3.03E+17	138.446	9.915616

Table 8 Results for target 4 with 2% Tc content, totaling 123 kg of Tc

Incident Energy (MeV)	Energy Per Transmutation (MeV)	Transmutation rate (atoms/s)	Initial halflife (years)	Transmutations per Tc99 atom produced
700	73.82652	2.03E+17	81.25837	6.650704
750	71.90757	2.08E+17	79.14625	6.828187
800	70.34794	2.13E+17	77.42962	6.979569
850	68.21949	2.2E+17	75.0869	7.197332
900	66.8746	2.24E+17	73.60662	7.342076
950	66.26227	2.26E+17	72.93265	7.409924
1000	65.17681	2.3E+17	71.73793	7.533329
1050	64.80862	2.31E+17	71.33267	7.576128
1100	63.81956	2.35E+17	70.24405	7.69354
1150	63.93861	2.34E+17	70.37508	7.679215
1200	63.12814	2.37E+17	69.48302	7.777805

The 123 kg of technetium used in the 2% Tc content version of target 4 is a more reasonable amount, and yields the shortest effective halflife, but the energy required per transmutation is markedly higher. A different geometry with a similar Tc content but a lower energy requirement per transmutation would improve the system. Target 5 was designed to attempt to achieve this. The target length was reduced from 150 cm to 120 cm, the radius reduced from 50 cm to 40 cm, the hole depth was reduced from 40 cm to 30 cm, and the hole radius reduced from 12 cm to 10 cm. The reflector was 40 cm thick around the radius of the target, 50 cm thick in the direction of the beam and 80 cm thick on the back of the target, to improve the reflection of the forward momentum biased particles. The total Tc-lead volume in target 5 is 593671 cm^3, down almost 50% from target 4's volume of 1159967 cm^3. Using 5% Tc content in target 5 gives a total Tc mass of 131 kg, which is close to the 123 kg mass in the 2% version of target 4. The results for target 5 with 5% Tc are shown in Table 9.

Table 9 Results for target 5 with 5% Tc content, totaling 131 kg of Tc

Incident Energy (MeV)	Energy Per Transmutation (MeV)	Transmutation rate (atoms/s)	Initial halflife (years)	Transmutations per Tc99 atom produced
700	65.78367	2.28E+17	77.10498	7.463833
750	64.59256	2.32E+17	75.70888	7.601469
800	62.86308	2.38E+17	73.68176	7.810599
850	61.4236	2.44E+17	71.99455	7.993643
900	59.98478	2.5E+17	70.30811	8.185382
950	59.37581	2.52E+17	69.59434	8.269333
1000	58.31116	2.57E+17	68.34646	8.420315
1050	58.05934	2.58E+17	68.0513	8.456837
1100	57.56056	2.6E+17	67.46668	8.530118
1150	57.78753	2.59E+17	67.73271	8.496615
1200	56.93819	2.63E+17	66.7372	8.623357

The energy required per transmutation is lower here than in the 2% target 4 model, and the initial halflife of the Tc in the target is shorter. This shows some improvement in both parameters, though the difference is relatively small. Further design alterations and iterations could reduce the energy requirements and effective halflife further. Also, increasing the beam power should cause a proportional increase in the transmutation rate and decrease in the halflife, without changing the efficiency parameters, so long as the beam still operates the same way and thermal issues with the increased rate of heat transfer to the target do not arise.

4. CONCLUSION

4.1 Summary of results and comparison to other systems

^{99}Tc was selected as the best LLFP to transmute for waste reduction purposes. The reference accelerator power was 2.4 MW. The final target design selected was target 5. The central target region consisted of a mixture of natural lead and ^{99}Tc with a 5% technetium content by atom. The density was 11 g/cm^3, and the total volume was 1159967 cm^3, resulting in a total mass of 131kg of technetium in the target. The technetium-lead region is a cylinder with a radius of 40 cm and a length of 120 cm. A cylindrical hole with a radius of 10 cm and a depth of 30 cm was removed from one face of the target to allow the beam to impact nearer to the center of the target. A cylindrical graphite reflector extended 40 cm from the target radially, 80 cm from the back of the target and 50 cm from the front of the target, with a matching cylindrical hole for the beam.

The optimal incident particle energy tested for this target was 1200 MeV. The resulting input particle energy required per technetium nuclide transmuted was 56.9 MeV per transmutation. The initial effective halflife of the technetium in the system was 66.7 years. Other target designs had slightly lower input energy requirements per transmutation, but higher technetium mass requirements and longer effective halflives. This system slightly under performs a different study on transmuting ^{99}Tc with an accelerator that obtained a transmutation energy of 29 MeV with an effective halflife of 5 years, using a much higher power (450 MW electric) beam and a similar spallation

neutron method. [11] This discrepancy could be due to different measuring methods and system designs.

The potential impact of transmuting ^{99}Tc on spent fuel storage is small while actinides remain the largest contributor to the heat production in spent fuel. If the actinides were removed, transmuting the technetium would have a significant impact on reducing the heat loading beyond 300 years for the remaining fission product containing waste. The final target design with the 2.4 MW accelerator would remove 1.36 kg of ^{99}Tc per, which corresponds to .0407 Watts of long term decay heat generation from the spent fuel inventory per year of operation. The total mass is 131 kg, so this destroys 1.04% of the ^{99}Tc per year initially. With an approximate accelerator efficiency of 50%, this would require pumping 4.8 MW of electricity into an accelerator constantly to transmute 1.36 kg of technetium into Ruthenium per year.

For comparison, another study done estimates that a system placing 316.7 kg of ^{99}Tc in the reflector region of a sodium cooled ATW core achieve a 36.5% burnup in the ^{99}Tc at discharge, corresponding to a destruction rate of 27.2 kg, or 7.03% of the technetium in their system per year. [5] The use of a reactor to produce neutrons can yield much higher fluxes and therefore higher transmutation rates.

4.2 Further work and recommendations

The design could be improved by performing further iterations on the dimensions and technetium content of the target, and a wider range of beam energies could be run to possibly improve the parameters for some target designs.

Transmuting fission products in a non fissioning accelerator based system is not an effective option for reducing the radioactivity of spent fuel. The impact on the waste is far too small compared to the energy requirements without the presence of an energy source that is effectively free and infinite.

REFERENCES

[1] K. Yancey, "Nationwide Used Fuel Inventory Analysis," MS Thesis, Texas A&M University, Department of Nuclear Engineering, 2013.

[2] A. Stanculescu, "IAEA activities in the area of partitioning and transmutation," *Nuclear Instruments and Methods in Physics,* vol. 562, no. 2, pp. 614-617, 2006.

[3] A. C. Muller, "Transmutation of nuclear waste and the future MYRRHA demonstrator," 12059, in *11th International Conference on Nucleus-Nucleus Collisions*, San Antonio TX, 2012.

[4] V. Peretroukhine, V. Radchenkob, A. Kozar, V. Tarasov, I. Toporov, K. Rotmanov, L. Lebedeva, S. Rovny and V. Ershov, "Technetium transmutation and production of artificial stable ruthenium," *Comptes Rendus Chimie,* vol. 7, no. 12, pp. 1215-1218, 2004.

[5] W. S. Yang, Y. Kim, R. N. Hill, T. A. Taiwo and H. S. Khalil, "Long-lived fission product transmutation studies," *Nuclear Science and Engineering,* vol. 146, pp. 291-318, 2004.

[6] N. Amrani, "Transmutation of the radiotoxic isotope 99Tc under irradiation in the BR2 high flux reactor," *Annals of Nuclear Energy,* vol. 38, no. 6, pp. 1347-1350, 2011.

[7] K. Kawashima, K. Kobayashi and K. Kaneto, "Utilization of fast reactor excess neutrons for burning long lived fission products," *Progress in Nuclear Energy,* vol. 29, no. Supplement, pp. 281-288, 1995.

[8] N. Demir, G. Genc, T. Altunok and H. Yapici, "Rapid transmutation of high-level nuclear wastes in a catalyzed fusion-driven system," *Journal of Fusion Energy,* vol. 28, no. 1, pp. 107-117, 2009.

[9] A. Abanades, F. Alvarez-Velarde, E. M. Gonzalez-Romero, K. Ismailov, A. Lafuente, M. Nishihara, M. Saito, A. Stanculescu and T. Sugawara, "Monte Carlo analysis of the long-lived fission product neutron captue rates at the Transmutation by Adiabatic Resonance Crossing (TARC) experiment," *Nuclear Engineering and Design,* vol. 245, pp. 148-153, 2013.

[10] W. S. Park, Y. H. Kim, C. K. Park, J. S. Chung and C. H. Kim, "A design study for 99Tc and 129I transmutation in the HYPER system," *Nuclear Science and Engineering,* vol. 143, no. 2, pp. 188-201, 2003.

[11] T. Kase and K. Konashi, "Transmutation of 99Tc with the use of an accelerator," *Nuclear Science and Engineering,* vol. 118, no. 3, pp. 153-159, 1994.

[12] J.-L. Bairrotte, S. Bousson, T. Junquera, A. C. Mueller and A. Olivier, "A reference accelerator scheme for ADS applications," *Nuclear Instruments and Methods in Physics,* vol. 562, no. 2, pp. 656-661, 2006.

[13] National Nuclear Data Center, *Chart of the nuclides,* Upton, New York: Brookhaven National Laboratory, 2014.

[14] D. Rochman, S. Herman, S. F. Mughabghab and P. Oblozinska, "New evaluation of the 99Tc neutron-induced cross sections for the ENDF/B-VII.0 library," *Nuclear Science and Engineering,* vol. 158, no. 1, pp. 68-77, 2008.

APPENDIX A

CROSS SECTION DATA TABLES

Total neutron interaction cross sections other than capture or scattering

E (MeV)	sigma (b)	E (MeV)	sigma (b)	E (MeV)	sigma (b)	E (MeV)	sigma (b)
8.8	0	12.3	1.031544	23	1.735436	58	1.413462
8.9	0	12.4	1.05836	24	1.713668	59	1.408341
9	0	12.5	1.085295	25	1.701393	60	1.403463
9.1	0.001525	12.6	1.109612	26	1.688956	80	1.363939
9.2	0.015808	12.7	1.131142	27	1.676812	100	1.291311
9.3	0.032615	12.8	1.152528	28	1.665035	120	1.213328
9.4	0.049779	12.9	1.174108	29	1.653165	140	1.146689
9.5	0.066842	13	1.195591	30	1.641436	160	1.072798
9.6	0.094179	13.1	1.21514	31	1.62976	180	1.035614
9.7	0.13187	13.2	1.23286	32	1.61841	200	1.030469
9.8	0.169517	13.3	1.250324	33	1.607008	220	1.0275
9.9	0.207286	13.4	1.267927	34	1.595701	240	1.026294
10	0.244917	13.5	1.285569	35	1.585048	260	1.026796
10.1	0.28342	13.6	1.301691	36	1.57519	280	1.027965
10.2	0.323181	13.7	1.316336	37	1.565238	300	1.029823
10.3	0.363112	13.8	1.330958	38	1.555524	320	1.03228
10.4	0.40302	13.9	1.345383	39	1.546118	340	1.034752
10.5	0.443045	14	1.360126	40	1.536875	360	1.037437
10.6	0.481363	14.1	1.373212	41	1.528218	380	1.040962
10.7	0.518508	14.2	1.384705	42	1.519739	400	1.044231
10.8	0.555675	14.3	1.396268	43	1.511692	420	1.044384
10.9	0.592619	14.4	1.407792	44	1.503701	440	1.047284
11	0.629587	14.5	1.419389	45	1.495968	460	1.050584
11.1	0.629736	14.6	1.431122	46	1.488587	480	1.052984
11.2	0.665625	14.7	1.442624	47	1.481467	500	1.054284
11.3	0.700398	14.8	1.454185	48	1.474373	520	1.059384
11.4	0.735082	14.9	1.46566	49	1.467385	540	1.062584
11.5	0.770016	15	1.477399	50	1.460615	560	1.067984
11.6	0.805131	16	1.516287	51	1.454092	580	1.073084
11.7	0.836889	17	1.552919	52	1.447857	600	1.074084
11.8	0.865018	18	1.604381	53	1.441664	620	1.078284
11.9	0.922138	19	1.624208	54	1.435203	640	1.082284
12	0.950636	20	1.638906	55	1.429496	660	1.084584
12.1	0.978301	21	1.742518	56	1.424112	680	1.089084
12.2	1.005074	22	1.735436	57	1.418717	700	1.093684

Total neutron interaction cross sections other than capture or scattering continued

E (MeV)	sigma (b)	E (MeV)	sigma (b)
720	1.095584	1420	1.114943
740	1.098184	1440	1.114754
760	1.100184	1460	1.114514
780	1.101184	1480	1.114239
800	1.103684	1500	1.11403
820	1.107184		
840	1.109384		
860	1.112484		
880	1.113684		
900	1.114284		
920	1.115384		
940	1.119784		
960	1.121284		
980	1.122084		
1000	1.122984		
1020	1.125484		
1040	1.125684		
1060	1.125884		
1080	1.126484		
1100	1.128184		
1120	1.128884		
1140	1.128484		
1160	1.130084		
1180	1.130384		
1200	1.130784		
1220	1.115001		
1240	1.115157		
1260	1.115351		
1280	1.115453		
1300	1.115493		
1320	1.115509		
1340	1.115438		
1360	1.115352		
1380	1.115303		
1400	1.115149		

Total proton nuclear interaction cross sections

E (MeV)	sigma (b)	E (MeV)	sigma (b)	E (MeV)	sigma (b)	E (MeV)	sigma (b)
1	4.12E-11	90	1.127252	720	1.0531	1420	1.071894
2	3.77E-06	100	1.102454	740	1.0568	1440	1.07194
3	0.000476	110	1.080989	760	1.0591	1460	1.072229
4	0.007667	120	1.062202	780	1.0616	1480	1.072365
5	0.046823	130	1.046013	800	1.0651	1500	1.072516
6	0.153017	140	1.031677	820	1.0668		
7	0.306835	150	1.018649	840	1.0686		
8	0.453447	160	1.00729	860	1.0718		
9	0.576031	180	0.987361	880	1.0739		
10	0.67444	200	0.970346	900	1.0755		
11	0.756036	220	1.0099	920	1.0776		
12	0.828099	240	1.0122	940	1.08		
13	0.890711	260	1.0154	960	1.0815		
14	0.942091	280	1.0128	980	1.0835		
15	0.983099	300	1.0155	1000	1.0836		
16	1.017158	320	1.0191	1020	1.0846		
17	1.046772	340	1.0212	1040	1.0867		
18	1.073177	360	1.0263	1060	1.0875		
19	1.09772	380	1.031	1080	1.0898		
20	1.120498	400	1.0334	1100	1.0904		
22	1.163876	420	0.9886	1120	1.0906		
24	1.201201	440	0.9966	1140	1.0913		
26	1.229436	460	1.0017	1160	1.0927		
28	1.248396	480	1.0043	1180	1.0926		
30	1.260454	500	1.0104	1200	1.0934		
35	1.28253	520	1.0165	1220	1.067636		
40	1.286651	540	1.0204	1240	1.068341		
45	1.278523	560	1.0256	1260	1.068958		
50	1.261939	580	1.0291	1280	1.06949		
55	1.241049	600	1.0328	1300	1.069942		
60	1.22594	620	1.0365	1320	1.07048		
65	1.205704	640	1.0386	1340	1.07083		
70	1.189514	660	1.0423	1360	1.071179		
75	1.170808	680	1.0448	1380	1.071479		
80	1.156483	700	1.0478	1400	1.07173		

APPENDIX B

TABLES OF COLLECTED DATA

Table 10 Data for transmutation efficiencies obtained using MCNPX model of protons in an infinite pure CsI target

Incident Energy (MeV)	Particles run	Proton interactions	Neutron interactions	Total	Energy/ trans (MeV)
200	10000	2472	20308	22780	87.79631255
300	10000	4398	47549	51947	57.75116946
400	10000	6412	86640	93052	42.9867171
500	10000	8205	128388	136593	36.60509689
600	10000	9733	173406	183139	32.76200045
700	10000	10889	217928	228817	30.59213258
800	10000	11997	265611	277608	28.81761333
900	10000	12886	308553	321439	27.99909159
1000	10000	13733	355147	368880	27.10908697
1100	10000	14371	396621	410992	26.76451123
1200	10000	15070	440219	455289	26.35688541
1300	10000	15495	474764	490259	26.51659633
1400	10000	16209	513636	529845	26.42282177
1500	10000	16668	548435	565103	26.5438336
1600	10000	17104	587282	604386	26.47314796
1700	10000	17525	622439	639964	26.56399422
1800	10000	17858	649588	667446	26.96847385
1900	10000	18307	685609	703916	26.99185698
2000	10000	18805	725255	744060	26.87955272

Table 11 Data for the average beam energy required per target nuclide transmuted for different incident particles

Incident Energy (MeV)	Proton Energy/ trans (MeV)	Deuteron Energy/ trans (MeV)	Alpha Energy/ trans (MeV)
400	57.75	40.48	215.15
500	42.99	34.39	147.97
600	36.61	29.63	116.90
700	32.76	30.01	94.05
800	30.59	26.02	81.40
900	28.82	25.09	69.16
1000	28.00	24.45	91.03
1100	27.11	24.08	57.30
1200	26.76	23.92	52.60
1300	26.36	23.79	49.13
1400	26.52	23.88	45.83
1500	26.42	23.74	43.71
1600	26.54	24.93	41.23
1700	26.47	23.85	39.67
1800	26.56	24.05	38.61
1900	26.97	24.46	37.00
2000	26.99	25.33	36.45